Fabrication of nanopores in 1 nm thick carbon nanomembranes with slow highly charged ions

Robert Ritter,[1] Richard A. Wilhelm,[2,3] Michael Stöger-Pollach,[4] René Heller,[2] Arndt Mücklich,[2] Udo Werner,[5] Henning Vieker,[5] André Beyer,[5] Stefan Facsko,[2] Armin Gölzhäuser,[5] and Friedrich Aumayr[1,a)]
[1]*Institute of Applied Physics, TU Wien-Vienna University of Technology, 1040 Vienna, Austria*
[2]*Institute of Ion Beam Physics & Materials Research, Helmholtz-Zentrum Dresden-Rossendorf, 01328 Dresden, Germany*
[3]*Technische Universität Dresden, 01062 Dresden, Germany*
[4]*USTEM, TU Wien-Vienna University of Technology, 1040 Vienna, Austria*
[5]*Fakultät für Physik, Universität Bielefeld, 33615 Bielefeld, Germany*

(Received 6 November 2012; accepted 4 February 2013; published online 14 February 2013)

We describe the use of slow highly charged ions as a simple tool for the fabrication of nanopores with well-defined diameters typically between 10 and 20 nm in freestanding, 1 nm thick carbon nanomembranes (CNMs). When CNMs are exposed to a flux of highly charged ions, for example Xe^{40+}, each individual ion creates a circular nanopore, the size of which depends on the kinetic and potential energy of the impinging ion. The controlled fabrication of nanopores with a uniform size opens a path for the application of CNM based filters in nanobiotechnology. © *2013 American Institute of Physics*. [http://dx.doi.org/10.1063/1.4792511]

Research on nanolayers, i.e., extremely thin films with a thickness below 10 nm, is a fast growing area within nanoscience and technology. Ignited by the discovery of graphene, which is—most likely—the thinnest mechanically stable two-dimensional material, engineered nanolayers currently receive an enormous attention, and a variety of two-dimensional nanostructures are currently developed and tested. Among them, carbon nanomembranes (CNMs) made from self-assembled monolayers (SAMs)[1] play a prominent role as they provide a modular construction system for diverse types of membranes.[2] CNMs are functional two-dimensional carbon materials; their thickness and other properties can be exactly tailored by an appropriate choice of the molecular precursors and the fabrication conditions. CNMs are made by radiation-induced cross-linking of surface bound self-assembled monolayers of aromatic molecules. The resulting two-dimensional polymeric film is then released from the substrate, cf. Fig. 1(a), and transferred onto arbitrary locations. CNMs show a high mechanical stability and can withstand pressures of up to ~1 bar[3,4] and can be freely suspended over openings and gaps that are more than 100 μm wide.[5,6] Fig. 1(b) shows a Helium ion microscopy (HIM) image of a 1 nm thick CNM that has been transferred onto a copper grid with hexagonal openings of ~60 μm width. Note that the free-standing CNM uniformly covers the entire grid, and that only one "membrane defect" is found in the lower part of the image (see arrow); here, a rupture in the CNM leaves an opening partly covered, which can act as a guide to the eye that nicely demonstrates the uniformity of this CNM. Fig 1(c) shows a higher magnification HIM image of a copper mesh covered by a CNM. Here, the CNM almost looks like "plastic foil" wrapped over a hexagonal copper rim. It can be stated that this intuitive picture of a CNM as a "nanoscale saran wrap" is quite reasonable; mechanical tests yielded a Young modulus of about 10 GPa, i.e., a typical value for polymer films.

CNMs share some similarity with graphene, as they are extremely thin carbon (~1 nm). However, in contrast to graphene, their surfaces can be easily chemically modified by chemical lithography[7] to produce functional 2D materials. The surfaces of CNMs can be engineered with complex architectures, such as patterns of proteins,[8] dyes,[9,10] or polymer brushes.[11,12] These customized CNMs have been used as microscopy supports,[5] nanosieves,[13] "Janus" membranes,[10] and layered structures.[14] Combining tailored CNMs with other different types of nanomembranes (graphene, sieves, and SiN) opens a path to engineer functional nanolayers for electronic, optical, lab-on-a-chip, and micro-/nanomechanical (MEMS/NEMS) devices.

In this work, we explore the perforation of CNMs with pores of uniform sizes, so they can be applied as sieves or filters. We use highly charged ions (HCI), i.e., atoms where the electrons are almost completely stripped resulting in positive ions with an electric charge q between 20+ and 40+ as a tool for pore fabrication. Studies on the interaction of slow ($v < v_{Bohr}$, E_{kin} in the keV range) HCI have been performed with a broad range of materials in recent years.[15,16] A particularly strong interest in the utilization of slow HCI as projectiles impacting solid surfaces has arisen from the distinct advantage that energy deposition and associated defect formation is limited to the topmost atomic layers. This is in stark contrast to the damage cascade initiated by swift (MeV–GeV) heavy ions. Here, a possible nanostructure formation at the surface is always accompanied by the formation of tracks, which can reach several hundreds of nm deep into the solid.[16,17]

For individual slow HCI, it has been found that their high potential energy alone, i.e., the sum of the binding energies of all missing electrons, can be sufficient to cause permanent damage on some materials, for example, nanosized

a)e-mail: aumayr@iap.tuwien.ac.at.

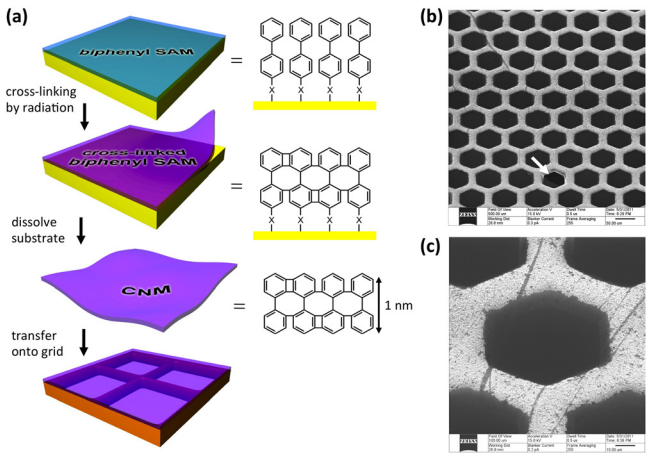

FIG. 1. (a) Schematic of CNM fabrication: a SAM of aromatic molecules, here biphenyls, is formed on a surface and cross-linked by radiation. After the supporting substrate is dissolved, a CNM with the thickness of the monolayer, here 1 nm, is generated and transferred onto a metal grid. (b) HIM image of a CNM that is placed free-standing on a Cu grid with hexagonal 60 μm wide meshes. (c) High magnification HIM image showing a CNM suspending over an opening in the Cu grid.

hillocks on a CaF_2 surface.[18] In this case, even approaching zero kinetic energy, every single ion produces a hillock, if the ion's potential energy exceeds a certain threshold value. In the case of CaF_2, this threshold could be linked to a solid-liquid phase transition. The existence of potential energy thresholds, above which observable topographic modifications can be achieved, seems to be a more general feature in slow HCI—solid interaction. Even so, latent material damage can set in at much lower potential energies. Recent studies on CaF_2[19] and BaF_2[20] show that areas structurally weakened by sub-threshold ion bombardment can be revealed in the form of triangular[19] or pyramidal[20] pits by exposure to a chemical etchant.

The appearance of nanostructures induced by slow HCI depends on the target material properties and, as a consequence thereof, on how energy is dissipated in the surface-near region. So far, the found spectrum ranges from hillocks (CaF_2[18] and $SrTiO_3$[21]), pits, or craters (KBr,[22] PMMA,[23] and Si[24]), to caldera-type structures (TiO_2[25]) and regions of enhanced friction (HOPG[26] and mica[27]).

In the following, we present investigations on the effect of slow HCI irradiation on CNMs. Although, coming from a very different starting point as compared to a solid bulk material, we find that single slow HCI, because of their very localized energy deposition, are able to produce nanosized pores in the membranes, without creating further visible damage. Our results indicate that the pore size can be tuned (increased) with the potential energy, but also depends on the kinetic energy of the impacting ions.

For the irradiation of the CNMs, a source of the Dresden EBIT[28] (electron beam ion trap) type, located at Helmholtz-Zentrum Dresden-Rossendorf (HZDR), was employed, able to deliver Xe^{q+} ions in charge states of up to $q = 40$. The projectile ions could be extracted at voltages varying from 4500 V (no deceleration) down to below 100 V after passing a two-stage deceleration system.

Up to 4 CNMs (produced from biphenylthiol (BPT) and suspended on copper grids with a mesh width of 60 μm, purchased from CNM Technologies (Bielefeld, Germany)) at once were transferred to the target chamber in a standard scanning electron microscopy (SEM) holder and irradiated under normal incidence with charge states $20 \leq q \leq 40$ at varying kinetic energies (20–1400 eV/amu) and fluences (10^9–10^{10} ions/cm^2). After the irradiation procedure and with no further treatment, all CNMs were either immediately transferred to a transmission electron microscope (TEM) at HZDR (FEI TITAN 80-300 with image correction, 300 keV electron energy) or investigated at USTEM TU Wien (FEI TECNAI F20, 200 keV electron energy). TEM images of irradiated CNMs (see, Figs. 2(c) and 2(d) and insets in Fig. 3) clearly show that pores have been formed as a result of individual ion impact events. The respective number densities of found pores are in excellent agreement with the applied fluences, i.e., practically every individual slow HCI has left behind a pore on its passage through the membrane. Our TEM investigations show that for all employed combinations of potential energy (ion charge state) and kinetic energy, pores are formed in the membranes if the charge state exceeds 25+. Two irradiations with Xe^{21+} ions performed with both highest and lowest possible kinetic energies as well as irradiations with Xe projectiles in lower charge states did not yield any evidence for pore formation, indicating that a minimum potential energy (threshold) is necessary to achieve such. After the first observation of pores with TEM, a number of other microscopy techniques were employed (see, Fig. 2) to image ion-induced pores: HIM images of selected samples (Xe^{40+}, $E_{kin} = 180$ keV, Fig. 2(a) and Xe^{40+}, $E_{kin} = 4$ keV, Fig. 2(b)) were taken at the Universität Bielefeld using a Zeiss Orion Plus Helium Ion Microscope (35.7 kV He ion current of 0.5 pA). SEM images of a single sample (Xe^{40+}, $E_{kin} = 12$ keV, Figs. 2(e) and 2(f)) were taken at USTEM TU Wien with a FEI QANTA 200 FEG. Atomic force microscopy (AFM) images of selected samples (Xe^{35+}, $E_{kin} = 12$ keV, Figs. 2(g) and 2(h) and Xe^{40+}, $E_{kin} = 40$ keV) were recorded at IAP TU Wien with a CYPHER AFM (Asylum Research) operated under ambient conditions in intermittent contact mode with commercially available silicon cantilevers with a supersharp diamond-like carbon tip (nominal tip radius of 1 nm). Image display was performed with the WSXM software.[29]

For the determination of the potential energy dependence of the pore size, a series of irradiations (Xe^{q+}, $q = 20$, 25, 30, 35, and 40) was performed at a fixed kinetic energy (40 keV) for the impacting ions. For the acquisition of the size distribution of pores formed in CNMs, TEM images (since they were available for all charge states and offer high resolution) were displayed in IMAGEJ[30] and analyzed according to the following procedure: Pores in the images were magnified, marked, and subsequently analyzed regarding their area distribution with an automatic particle analysis. The mean diameter was then deducted assuming a circular shape for each imaged pore.

Our results give a strong indication for an increase of pore size with increasing potential energy (see, Fig. 3), apart from an apparent dip in the Xe^{35+} case. This dip has been reproduced in a second experiment and, for the moment, can be attributed to an inverse kinetic energy dependence in comparison to other charge states investigated in this study. While

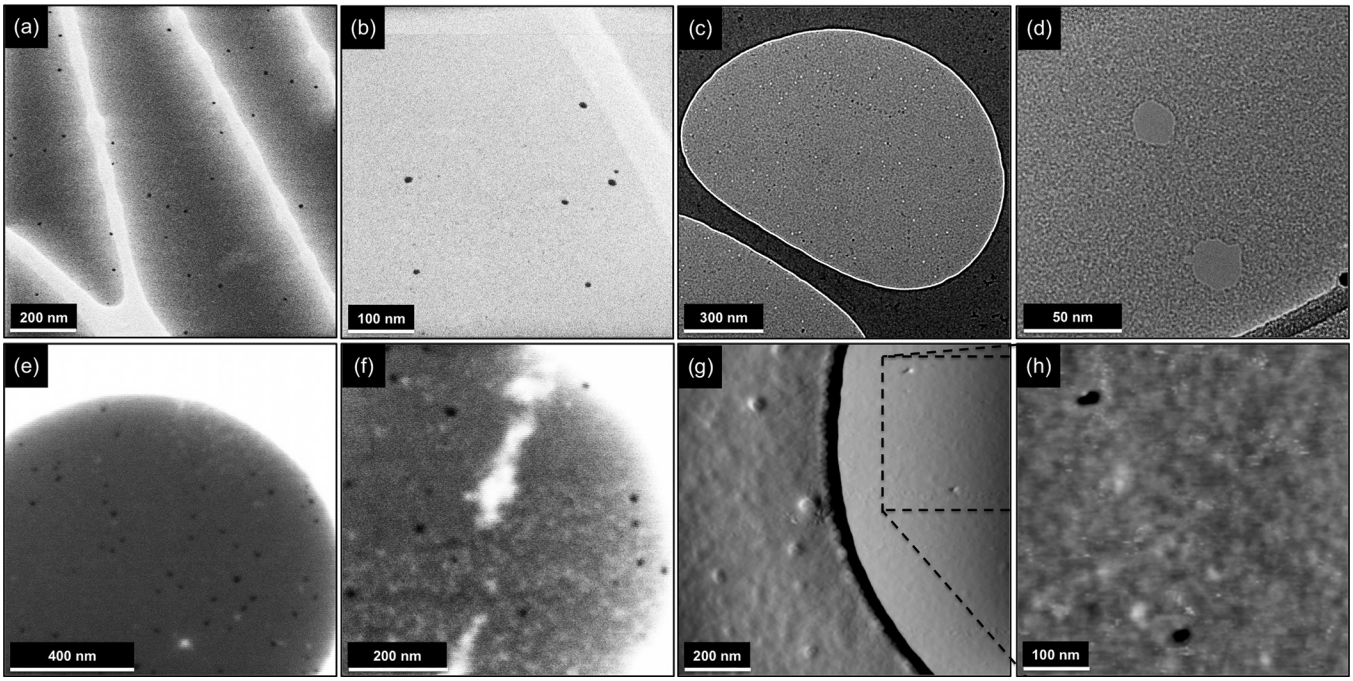

FIG. 2. Pores in CNMs imaged with different microscopy techniques after irradiation with slow highly charged ions; (a) HIM image of pores induced by Xe^{40+} ($E_{kin} = 180$ keV) ions. (b) HIM image, Xe^{40+} ($E_{kin} = 4$ keV). (c) TEM overview image, Xe^{40+} ($E_{kin} = 180$ keV). (d) TEM image, Xe^{40+} ($E_{kin} = 40$ keV). (e) and (f) SEM images, Xe^{40+} ($E_{kin} = 12$ keV). (g) AFM amplitude image, Xe^{35+} ($E_{kin} = 12$ keV). (h) AFM height image (zoomed in from (g)). While the TEM images pores as bright spots, with all other techniques (HIM, SEM, and AFM), they appear as dark spots.

the average pore size produced by an ion of a given charge state (e.g., Xe^{30+} and Xe^{40+}) tends to increase when the kinetic energy is raised, the opposite trend is observed for Xe^{35+} ions, i.e., slower ions induce larger pores. Thorough studies on the effect of kinetic energy variations are currently underway.

Comparing the above-described method to produce perforated CNMs with other schemes of nanopore fabrication, it becomes clear that highly charged ions are a very versatile drilling tool for ultra thin membranes. Basically, the membrane needs only be placed in the path of the ion and the ion produces a circular pore upon impact whose diameter is defined within a few nanometers. Neither resist material nor development steps are needed. Other CNM perforation procedures like EUV-interference lithography[13] have the drawback that they only work when the monolayer is still on a supporting substrate and need to be transferred to the desired location, while the HCI patterning can basically be performed *in situ*. Compared to conventional ion-induced drilling methods, like focused ion beam lithography (FIB) with Ga, Ne, or He ions, HCI patterning has the further advantage that each single impact produces one nanopore. In Helium ion beam lithography, for example, it was shown that the impact of about 100 He ions per square Å is not sufficient to mill away a freely suspended graphene membrane.[31] Furthermore, for reasonable exposure times, a much higher pore density (typically 10^9–10^{10}/cm^2) can be achieved with slow HCI as compared to a FIB.

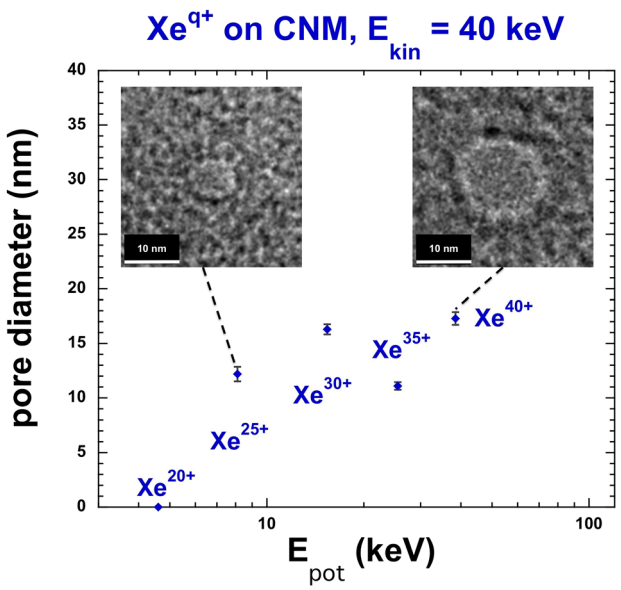

FIG. 3. Evolution of pore diameters in CNMs induced by slow HCIs as a function of ion potential energy: The pore diameter increases from threshold charge state (Xe^{25+}), to highest available charge state (Xe^{40+}) when the kinetic energy of the ions is left constant (40 keV). TEM images of single pores for these cases are displayed to illustrate the observed size increase.

The formation of nanopores in CNMs by slow HCI can qualitatively be understood as a consequence of the multiple neutralization and de-excitation processes taking place when a slow HCI approaches a surface (see, e.g., Refs. 32–35 and references therein). Many electrons from the target are transferred into highly excited states of the projectile ("hollow-atom" formation), and subsequently emitted via auto-ionization and other Auger processes.[32] Remaining unbalanced holes cause structural weakening of the target. The Auger decay of the hollow atom leads to the emission of electrons with low to intermediate energies up to a few hundred eV.[32,33] Part of the ion's potential energy stored in the incoming HCI will thus be deposited in the form of many holes and electron-hole pairs in the CNM.

For charge states below but close to the determined threshold of 25+ ($E_{pot} = 8.1$ keV), e.g., Xe^{21+}, even at kinetic energies ($E_{kin} = 94$ keV, dE/dx = 2.45 keV/nm) close to the nuclear stopping power maximum ($E_{kin} = 160$ keV and dE/dx = 2.95 keV/nm) derived from stopping and range of ions in matter (SRIM)[36] calculations, no pores have been observed after irradiation. Besides this fact, the time for the ion to pass the membrane in our experiments is between 2 fs (highest kinetic energy of 180 keV) and 14 fs (lowest kinetic energy of 3.3 keV), which is lower than the neutralization time for HCIs in carbon materials of ca. 10 fs.[33] For the presented potential energy series at a fixed kinetic energy of 40 keV (see, Fig. 3), ions require only 4 fs for passage through the membrane. Additional interaction processes will take place well before contact and after exiting the membrane, as predicted by the "classical over-the-barrier model,"[37] but the ion will remain far from neutral. This leads to the conclusion that the potential energy is (especially for short times) only partially deposited in the material and also the electronic stopping power might be significantly higher than the average value taken from SRIM, since SRIM uses the equilibrium charge state (neutral in the employed E_{kin} regime), but the actual charge state remains far from equilibrium within the CNM. The influence of varying kinetic energies, which is still subject to discussion, might be strongly connected to this effect of partial potential energy deposition and enhanced electronic stopping in the far-from-equilibrium-regime. The kinetic energy of the projectile further determines the depth within which the de-excitation of the projectile is completed. Simulations on CaF_2 calculate this depth to ~1 nm for 150 q eV (= 4.5 keV for q = 30) and to ~4 nm for 10 q keV (= 300 keV for q = 30) Xe^{q+} projectiles (see, Fig. 4 of Ref. 18). In regions where the ionization density exceeds a certain critical value (threshold), fragments of the membrane are no longer bound and can be ejected or desorbed from the target surface.[17,23]

We consider two theoretical models for pore formation in the CNMs: Coulomb explosion,[38] i.e., kinetic energy transfer to target atoms after the explosion of an area strongly depleted of charge as a result of electron emission processes, could play a role in our experiments, although it has been ruled out as a mechanism for electronic sputtering for Xe charge states below 25.[35] As of now, however, it was not possible to analyze ejected fragments of the membrane. A considerable yield of charged fragments would be a strong indication for Coulomb explosion. Second, sputtering by intense, ultrafast electronic excitations is considered. This model was originally developed to describe structural instabilities in covalent solids due to the creation of a dense electron-hole plasma induced by femtosecond laser irradiation,[39,40] but has also shown validity in slow HCI ion surface interaction.[41] Structural instabilities arise directly from the promotion of electrons from the bonding valence band state to an anti-bonding state in the conduction band. Each electron-hole excitation causes a repulsive force between atoms[33] and can eventually result in material rupture.

In summary, we have shown that 1 nm thick CNMs are susceptible to damage creation by individual slow HCI. Impacts of Xe^{q+} ions in charge states $q \geq 25$ induce nanoscopic pores in the membranes, which have been imaged by a multitude of high resolution imaging techniques. Pores with diameters ranging from 30 nm down to only 3 nm have been observed and analyzed. For a fixed impact energy, the pore diameter increases with the potential energy of the HCI. The dependence of the pore size on the kinetic energy of the incident ions is still subject to studies and discussions.

While, in this work, we have focused mainly on the general aspects of pore production with slow HCI and possible imaging techniques, we are convinced that the continued work on this subject in the near future will lead to (a) a better understanding of the underlying mechanisms and (b) adaptable pore sizes, which can be fine-tuned by ion beam parameters. Once this knowledge has been established, CNMs treated with slow HCI might become of interest for use as nanosieves in a broad range of scientific applications. Nanopores formed in conducting CNMs[3] might also hold promise for studies on DNA translocation[42] and sequencing.

R.R. is a recipient of a DOC-fellowship of the Austrian Academy of Sciences. The Deutsche Forschungsgemeinschaft (DFG) is gratefully acknowledged for financial support under Project No. HE 6174/1-1. This work has been supported by the European Community as an Integrating Activity "Support of Public and Industrial Research Using Ion Beam Technology (SPIRIT)" under EC Contract No. 227012. Support from EURATOM-ÖAW and the Austrian FWF is acknowledged. A.B. and A.G. acknowledge financial support from the Volkswagenstiftung and the Deutsche Forschungsgemeinschaft (SFB 613).

[1]W. Eck, A. Küller, M. Grunze, B. Völkel, and A. Gölzhäuser, Adv. Mater. **17**, 2583 (2005).
[2]A. Turchanin and A. Gölzhäuser, Prog. Surf. Sci. **87**, 108 (2012).
[3]A. Turchanin, A. Beyer, C. T. Nottbohm, X. Zhang, R. Stosch, A. S. Sologubenko, J. Mayer, P. Hinze, T. Weimann, and A. Gölzhäuser, Adv. Mater. **21**, 1233 (2009).
[4]X. Zhang, A. Beyer, and A. Gölzhäuser, Beilstein J. Nanotechnol. **2**, 826 (2011).
[5]C. T. Nottbohm, A. Beyer, A. S. Sologubenko, I. Ennen, A. Hutten, H. Rosner, W. Eck, J. Mayer, and A. Gölzhäuser, Ultramicroscopy **108**, 885 (2008).
[6]A. Gölzhäuser and C. Wöll, ChemPhysChem **11**, 3201 (2010).
[7]A. Beyer, A. Godt, I. Amin, C. T. Nottbohm, C. Schmidt, J. Zhao, and A. Gölzhäuser, Phys. Chem. Chem. Phys. **10**, 7233 (2008).
[8]A. Turchanin, A. Tinazli, M. El-Desawy, H. Großmann, M. Schnietz, H. H. Solak, R. Tampé, and A. Gölzhäuser, Adv. Mater. **20**, 471 (2008).
[9]A. Biebricher, A. Paul, P. Tinnefeld, A. Gölzhäuser, and M. Sauer, J. Biotechnol. **112**, 97 (2004).
[10]Z. Zheng, C. T. Nottbohm, A. Turchanin, H. Muzik, A. Beyer, M. Heilemann, M. Sauer, and A. Gölzhäuser, Angew. Chem., Int. Ed. **49**, 8493 (2010).
[11]I. Amin, M. Steenackers, N. Zhang, A. Beyer, X. Zhang, T. Pirzer, T. Hugel, R. Jordan, and A. Gölzhäuser, Small **6**, 1623 (2010).
[12]I. Amin, M. Steenackers, N. Zhang, R. Schubel, A. Beyer, A. Gölzhäuser, and R. Jordan, Small **7**, 683 (2011).
[13]M. Schnietz, A. Turchanin, C. T. Nottbohm, A. Beyer, H. H. Solak, P. Hinze, T. Weimann, and A. Gölzhäuser, Small **5**, 2651 (2009).
[14]C. T. Nottbohm, A. Turchanin, A. Beyer, R. Stosch, and A. Gölzhäuser, Small **7**, 874 (2011).
[15]F. Aumayr, A. S. El-Said, and W. Meissl, Nucl. Instrum. Methods Phys. Res. B **266**, 2729 (2008).
[16]F. Aumayr, S. Facsko, A. S. El-Said, C. Trautmann, and M. Schleberger, J. Phys.: Condens. Matter **23**, 393001 (2011).
[17]L. Chadderton, Radiat. Meas. **36**, 13 (2003).
[18]A. S. El-Said, R. Heller, W. Meissl, R. Ritter, S. Facsko, C. Lemell, B. Solleder, I. C. Gebeshuber, G. Betz, M. Toulemonde, W. Moller, J. Burgdörfer, and F. Aumayr, Phys. Rev. Lett. **100**, 237601 (2008).
[19]A. S. El-Said, R. A. Wilhelm, R. Heller, S. Facsko, C. Lemell, G. Wachter, J. Burgdörfer, R. Ritter, and F. Aumayr, Phys. Rev. Lett. **109**, 117602 (2012).

[20]A. S. El-Said, R. Heller, F. Aumayr, and S. Facsko, Phys. Rev. B **82**, 033403 (2010).
[21]T. Peters, C. Haake, J. Hopster, V. Sokolovsky, A. Wucher, and M. Schleberger, Nucl. Instrum. Methods Phys. Res. B **267**, 687 (2009).
[22]R. Heller, S. Facsko, R. A. Wilhelm, and W. Möller, Phys. Rev. Lett. **101**, 096102 (2008).
[23]R. Ritter, R. A. Wilhelm, R. Ginzel, G. Kowarik, R. Heller, A. S. El-Said, R. M. Papaléo, W. Rupp, J. R. Crespo López-Urrutia, J. Ullrich, S. Facsko, and F. Aumayr, EPL **97**, 13001 (2012).
[24]M. Tona, H. Watanabe, S. Takahashi, N. Nakamura, N. Yoshiyasu, M. Sakurai, T. Terui, S. Mashiko, C. Yamada, and S. Ohtani, Surf. Sci. **601**, 723 (2007).
[25]M. Tona, Y. Fujita, C. Yamada, and S. Ohtani, Phys. Rev. B **77**, 155427 (2008).
[26]R. Ritter, G. Kowarik, W. Meissl, L. Süss, L. Maunoury, H. Lebius, C. Dufour, M. Toulemonde, and F. Aumayr, Nucl. Instrum. Methods Phys. Res. B **268**, 2897 (2010).
[27]R. Ritter, G. Kowarik, W. Meissl, A. S. El-Said, L. Maunoury, H. Lebius, C. Dufour, M. Toulemonde, and F. Aumayr, Vacuum **84**, 1062 (2010).
[28]F. Grossmann, R. Heller, M. Kreller, U. Kentsch, S. Landgraf, V. P. Ovsyannikov, M. Schmidt, F. Ullmann, and G. Zschornack, Nucl. Instrum. Methods Phys. Res. B **256**, 565 (2007).
[29]I. Horcas, R. Fernandez, J. M. Gomez-Rodriguez, J. Colchero, J. Gomez-Herrero, and A. M. Baro, Rev. Sci. Instrum. **78**, 013705 (2007).
[30]M. D. Abramoff, P. J. Magalhaes, and S. J. Ram, Biophoton. Int. **11**, 36 (2004), available at: http://igitur-archive.library.uu.nl/med/2011-0512-200507/ImageJ.pdf.
[31]M. C. Lemme, D. C. Bell, J. R. Williams, L. A. Stern, B. W. H. Baugher, P. Jarillo-Herrero, and C. M. Marcus, ACS Nano **3**, 2674 (2009).
[32]A. Arnau, F. Aumayr, P. M. Echenique, M. Grether, W. Heiland, J. Limburg, R. Morgenstern, P. Roncin, S. Schippers, R. Schuch, N. Stolterfoht, P. Varga, T. J. M. Zouros, and H. P. Winter, Surf. Sci. Rep. **27**, 117 (1997).
[33]T. Schenkel, A. V. Hamza, A. V. Barnes, and D. H. Schneider, Prog. Surf. Sci. **61**, 23 (1999).
[34]H. P. Winter and F. Aumayr, J. Phys. B **32**, R39 (1999).
[35]F. Aumayr and H. P. Winter, Philos. Trans. R. Soc. London **362**, 77 (2004).
[36]J. F. Ziegler, J. P. Biersack, and U. Littmark, *The Stopping and Range of Ions in Matter* (Pergamon, New York, 1985).
[37]J. Burgdörfer, P. Lerner, and F. W. Meyer, Phys. Rev. A **44**, 5674 (1991).
[38]I. S. Bitensky and E. S. Parilis, Nucl. Instrum. Methods Phys. Res. B **21**, 26 (1987).
[39]P. Stampfli, Nucl. Instrum. Methods Phys. Res. B **107**, 138 (1996).
[40]P. Stampfli and K. H. Bennemann, Appl. Phys. A **60**, 191 (1995).
[41]T. Schenkel, A. V. Hamza, A. V. Barnes, D. H. Schneider, J. C. Banks, and B. L. Doyle, Phys. Rev. Lett. **81**, 2590 (1998).
[42]C. A. Merchant, K. Healy, M. Wanunu, V. Ray, N. Peterman, J. Bartel, M. D. Fischbein, K. Venta, Z. Luo, A. T. C. Johnson, and M. Drindic, Nano Lett. **10**, 2915 (2010).